Weston Stacey
Nuclear Reactor Physics
John Wiley & Sons, 2001

6 Fuel Burnup

The long-term changes in the properties of a nuclear reactor over its lifetime are determined by the changes in composition due to fuel burnup and the manner in which these are compensated. The economics of nuclear power is strongly affected by the efficiency of fuel utilization to produce power, which in turn is affected by these long-term changes associated with fuel burnup. In this chapter we describe the changes in fuel composition that take place in an operating reactor and their effects on the reactor, the effects of the samarium and xenon fission products with large thermal neutron cross sections, the conversion of fertile material to fissionable material by neutron transmutation, the effects of using plutonium from spent fuel and from weapons surplus as fuel, the production of radioactive waste, the extraction of the residual energy from spent fuel, and the destruction of long-lived actinides.

6.1 CHANGES IN FUEL COMPOSITION

The initial composition of a fuel element will depend on the source of the fuel. For reactors operating on the uranium cycle, fuel developed directly from natural uranium will contain a mixture of ^{234}U, ^{235}U, and ^{238}U, with the fissile ^{235}U content varying from 0.72% (for natural uranium) to more than 90%, depending on the enrichment. Recycled fuel from reprocessing plants will also contain the various isotopes produced in the transmutation–decay process of uranium. Reactors operating on the thorium cycle will contain ^{232}Th and ^{233}U or ^{235}U, and if the fuel is from a reprocessing plant, isotopes produced in the transmutation–decay process of thorium.

During the operation of a nuclear reactor a number of changes occur in the composition of the fuel. The various fuel nuclei are transmuted by neutron capture and subsequent decay. For a uranium-fueled reactor, this process produces a variety of transuranic elements in the actinide series of the periodic table. For a thorium-fueled reactor, a number of uranium isotopes are produced. The fission event destroys a fissile nucleus, of course, and in the process produces two intermediate mass *fission products*. The fission products tend to be neutron-rich and subsequently decay by beta or neutron emission (usually accompanied by gamma emission) and undergo neutron capture to be transmuted into a heavier isotope, which itself undergoes radioactive decay and neutron transmutation, and so on. The fissile nuclei also undergo neutron transmutation via radiative capture

via radiative capture
followed by decay
or further transmutation

Fuel Transmutation–Decay Chains

Uranium-235, present 0.72% in natural uranium, is the only naturally occurring isotope that is fissionable by thermal neutrons. However, three other fissile (fissionable by thermal neutrons) isotopes of major interest as nuclear reactor fuel are produced as the result of transmutation–decay chains. Isotopes that can be converted to fissile isotopes by neutron transmutation and decay are known as *fertile isotopes*. ^{239}Pu and ^{241}Pu are products of the transmutation–decay chain beginning with the fertile isotope ^{238}U, and ^{233}U is a product of the transmutation–decay chain beginning with the fertile isotope ^{232}Th. These two transmutation–decay chains are shown in Fig. 6.1. Isotopes are in rows with horizontal arrows representing (n,γ) transmutation reactions, with the value of the cross section (in barns) shown. Downward arrows indicate β-decay, with the half-lives shown. Thermal neutron fission is represented by a dashed diagonal arrow, and the thermal cross

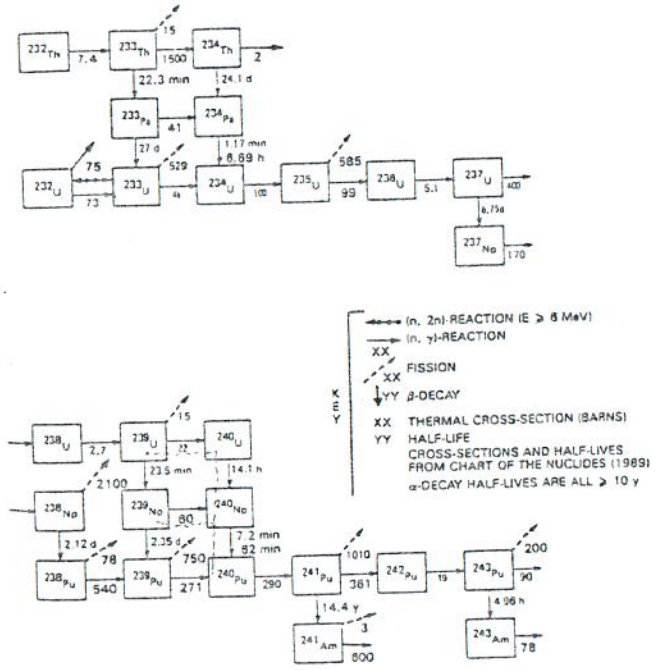

FIG 6.1

TABLE 6.1 Cross Section and Decay Data for Fuel Isotopes

Type	Abundance (%)	$t_{1/2}$	Decay Mode	Energy (MeV)	Spontaneous Fission Yield (%)	σ_γ^{th} (barns)	σ_f^{th} (barns)	RI_γ (barns)	RI_f (barns)	σ_γ^{χ} (barns)	σ_f^{χ} (barns)
Th	100	1.41×10^{10} y	α	4.1	$< 1 \times 10^{-9}$	7	—	84	—	0.09	0.08
Th	—	22.3 m	β	1.2	—	1285	13	643	11	0.09	0.11
Th	—	24.1 d	β	0.27	—	2	—	94	—	0.11	0.04
Pa	—	27.0 d	β	0.57	—	35	—	864	—	0.28	0.33
Pa	—	6.7 h	β	2.2	—	—	—	—	—	—	—
U	—	68.9 y	α	5.4	—	64	66	173	364	0.03	2.01
U	—	1.59×10^5 y	α	4.9	$< 6 \times 10^{-9}$	41	469	138	774	0.07	1.95
U	0.0057	2.46×10^5 y	α	4.9	1.7×10^{-9}	88	6	631	7	0.22	1.22
U	0.719	7.04×10^8 y	α	4.7	7.0×10^{-9}	87	507	133	278	0.09	1.24
U	—	2.34×10^6 y	α	4.6	9.6×10^{-8}	5	54	346	8	0.11	0.59
U	—	6.75 d	β	0.52	—	392	1	1084	49	0.93	0.74
U	99.27	4.47×10^9 y	α	4.3	5×10^{-5}	2	10	278	2	0.07	0.31
Np	—	23.5 m	β	1.3	—	—	—	—	—	—	—
Np	—	14.1 h	β	0.39	—	—	—	—	—	—	—
Pu	—	1.54×10^5 y	ec[a]	0.94	—	621	2453	259	1032	0.19	1.92
Pu	—		β[a]	0.49	—	—	—	—	—	—	—
Pu	—	2.14×10^6 y	α	5.0	$< 2 \times 10^{-10}$	144	20	661	7	0.17	1.33
Pu	—	2.12 d	β	1.3	—	399	1835	201	940	0.11	1.42

(Continued)

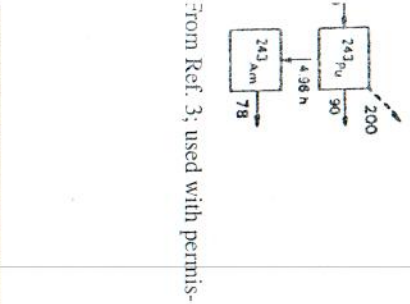

From Ref. 3; used with permis-

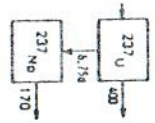

REACTION (E ≥ 6 MeV)
REACTION

MAL CROSS-SECTION (BARNS)
LIFE
S-SECTIONS AND HALF-LIVES
CHART OF THE NUCLIDES (1989)
AY HALF-LIVES ARE ALL ≥ 10 y

ne only naturally occurring
r, three other fissile (fission-
as nuclear reactor fuel are
. Isotopes that can be con-
decay are known as *fertile*
tion–decay chain beginning
of the transmutation–decay
e two transmutation–decay
horizontal arrows represent-
he cross section (in barns)
half-lives shown. Thermal
row, and the thermal cross

TABLE 6.1 Cross Section and Decay Data for Fuel Isotopes

Isotope	Abundance (%)	$t_{1/2}$	Decay Mode	Energy (MeV)	Spontaneous Fission Yield (%)	σ_γ^{th} (barns)	σ_f^{th} (barns)	RI_γ (barns)	RI_f (barns)	σ_γ^{χ} (barns)	σ_f^{χ} (barns)
^{232}Th	100	1.41×10^{10} y	α	4.1	$< 1 \times 10^{-9}$	7	—	84	—	0.09	0.08
^{233}Th	—	22.3 m	β	1.2	—	1285	13	643	11	0.09	0.11
^{234}Th	—	24.1 d	β	0.27	—	2	—	94	—	0.11	0.04
^{233}Pa	—	27.0 d	β	0.57	—	35	—	864	—	0.28	0.33
^{234}Pa	—	6.7 h	β	2.2	—	—	—	—	—	—	—
^{232}U	—	68.9 y	α	5.4	—	64	66	173	364	0.03	2.01
^{233}U	—	1.59×10^5 y	α	4.9	$< 6 \times 10^{-9}$	41	469	138	774	0.07	1.95
^{234}U	0.0057	2.46×10^5 y	α	4.9	1.7×10^{-9}	88	6	631	7	0.22	1.22
^{235}U	0.719	7.04×10^8 y	α	4.7	7.0×10^{-9}	87	507	133	278	0.09	1.24
^{236}U	—	2.34×10^6 y	α	4.6	9.6×10^{-8}	5	54	346	8	0.11	0.59
^{237}U	—	6.75 d	β	0.52	—	392	1	1084	49	0.93	0.74
^{238}U	99.27	4.47×10^9 y	α	4.3	5×10^{-5}	2	10	278	2	0.07	0.31
^{239}U	—	23.5 m	β	1.3	—	—	—	—	—	—	—
^{240}U	—	14.1 h	β	0.39	—	—	—	—	—	—	—
^{236}Np	—	1.54×10^5 y	ec[a]	0.94	—	621	2453	259	1032	0.19	1.92
			β[a]	0.49	—	—	—	—	—	—	—
^{237}Np	—	2.14×10^6 y	α	5.0	$< 2 \times 10^{-10}$	144	20	661	7	0.17	1.33
^{238}Np	—	2.12 d	β	1.3	—	399	1835	201	940	0.11	1.42

(Continued)

TABLE 6.1 *(Continued)*

Isotope	Abundance (%)	$t_{1/2}$	Decay Mode	Energy (MeV)	Spontaneous Fission Yield (%)	σ_γ^{th} (barns)	σ_f^{th} (barns)	RI_γ (barns)	Ri_f (barns)	σ_γ^{χ} (barns)	σ_f^{χ} (barns)
^{239}Np	—	236 d	β	0.72	—	33	—	445	—	0.19	1.46
^{240}Np	—	—	—	—	—	—	—	—	—	—	—
^{236}Pu	—	2.86 y	α	5.9	1.4×10^{-7}	126	146	401	59	0.15	2.08
^{237}Pu	—	45	ec	0.22	—	—	—	—	—	—	—
^{238}Pu	—	87.7 y	α	5.6	1.9×10^{-7}	458	15	154	33	0.10	1.99
^{239}Pu	—	2.41×10^4 y	α	5.2	3×10^{-10}	274	698	182	303	0.05	1.80
^{240}Pu	—	6.56×10^3 y	α	5.3	5.7×10^{-6}	264	53	8103	9	0.10	1.36
^{241}Pu	—	14.4 y	β	0.02	$< 2 \times 10^{-14}$	326	938	180	576	0.12	1.65
^{242}Pu	—	3.73×10^5 y	α	5.0	$> 5.5 \times 10^{-4}$	17	—	1130	—	0.09	1.13
^{241}Am	—	432 y	α	5.6	4×10^{-10}	532	3	1305	14	0.23	1.38

Source: Brookhaven National Laboratory Nuclear Data Center, *http://www.dne.bnl.gov/CoN/index.html.*

[a] 87.3% electron capture, 12.5% β.

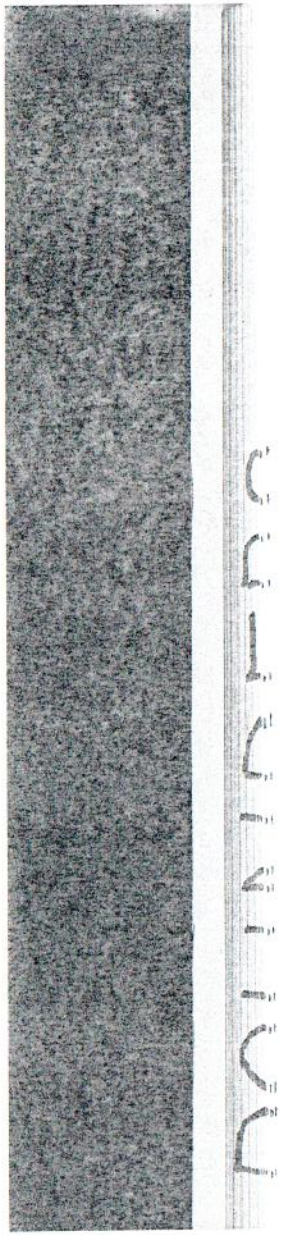

BLE 6.1 *(Continued)*

tope	Abundance (%)	$t_{1/2}$	Decay Mode	Energy (MeV)	Spontaneous Fission Yield (%)	σ_γ^{th} (barns)	σ_f^{th} (barns)	RI_γ (barns)	RI_f (barns)	σ_γ^χ (barns)	σ_f^χ (barns)
Np	—	236 d	β	0.72	—	33	—	445	—	0.19	1.46
Np	—	—	—	—	—	—	—	—	—	—	—
Pu	—	2.86 y	α	5.9	1.4×10^{-7}	126	146	401	59	0.15	2.08
Pu	—	45	ec	0.22	—	—	—	—	—	—	—
Pu	—	87.7 y	α	5.6	1.9×10^{-7}	458	15	154	33	0.10	1.99
Pu	—	2.41×10^4 y	α	5.2	3×10^{-10}	274	698	182	303	0.05	1.80
Pu	—	6.56×10^3 y	α	5.3	5.7×10^{-6}	264	53	8103	9	0.10	1.36
Pu	—	14.4 y	β	0.02	$< 2 \times 10^{-14}$	326	938	180	576	0.12	1.65
Pu	—	3.73×10^5 y	α	5.0	$> 5.5 \times 10^{-4}$	17	—	1130	—	0.09	1.13
Am	—	432 y	α	5.6	4×10^{-10}	532	3	1305	14	0.23	1.38

arce: Brookhaven National Laboratory Nuclear Data Center, *http://www.dne.bnl.gov/CoN/index.html*.
'.3% electron capture, 12.5% β.

section is shown. (Fast fission also occurs but is relatively less important in thermal reactors.) Natural abundances, decay half-lifes, modes of decay, decay energies, spontaneous fission yields, thermal capture and fission cross sections averaged over a Maxwellian distribution with $kT = 0.0253$ eV (σ^{th}), infinite-dilution capture and fission resonance integrals (RIs), and capture and fission cross sections averaged over the fission spectrum (σ^χ) are given in Table 6.1.

Fuel Depletion–Transmutation–Decay Equations

Concentrations of the various fuel isotopes in a reactor are described by a coupled set of production–destruction equations. We adopt the two-digit superscript convention for identifying isotopes in which the first digit is the last digit in the atomic number and the second digit is the last digit in the atomic mass. We represent the neutron reaction rate by $\sigma_x^{nm}\phi n^{nm}$, although the actual calculation may involve a sum over energy groups of such terms.

For reactors operating on the uranium cycle, the isotopic concentrations are described by

$$
\begin{aligned}
\frac{\partial n^{24}}{\partial t} &= -\sigma_a^{24}\phi n^{24} \\
\frac{\partial n^{25}}{\partial t} &= \sigma_\gamma^{24}\phi n^{24} - \sigma_a^{25}\phi n^{25} \\
\frac{\partial n^{26}}{\partial t} &= \sigma_\gamma^{25}\phi n^{25} - \sigma_a^{26}\phi n^{26} + \lambda_{ec}^{36} n^{36} \\
\frac{\partial n^{27}}{\partial t} &= \sigma_\gamma^{26}\phi n^{26} + \sigma_{n,2n}^{28}\phi n^{28} - \lambda^{27} n^{27} \\
\frac{\partial n^{28}}{\partial t} &= -\sigma_a^{28}\phi n^{28} \\
\frac{\partial n^{29}}{\partial t} &= \sigma_\gamma^{28}\phi n^{28} - (\lambda^{29} + \sigma_a^{29}\phi) n^{29} \\
\frac{\partial n^{36}}{\partial t} &= \sigma_{n,2n}^{37}\phi n^{37} - (\lambda^{36} + \sigma_a^{36}\phi) n^{36} \\
\frac{\partial n^{37}}{\partial t} &= \lambda^{27} n^{27} - \sigma_a^{27}\phi n^{37} \\
\frac{\partial n^{38}}{\partial t} &= \sigma_\gamma^{37}\phi n^{37} - (\lambda^{38} + \sigma_a^{38}\phi) n^{38} \\
\frac{\partial n^{39}}{\partial t} &= \lambda^{29} n^{29} - (\lambda^{39} + \sigma_a^{39}\phi) n^{39} \\
\frac{\partial n^{48}}{\partial t} &= \lambda^{38} n^{38} - \sigma_a^{48}\phi n^{48} \\
\frac{\partial n^{49}}{\partial t} &= \lambda^{39} n^{39} - \sigma_a^{49}\phi n^{49} + \sigma_\gamma^{48}\phi n^{48}
\end{aligned}
\tag{6.1}
$$

$$\frac{\partial n^{40}}{\partial t} = \sigma_\gamma^{39}\phi n^{39} - \sigma_a^{40}\phi n^{40} + \sigma_\gamma^{29}\phi n^{29} + \sigma_\gamma^{39}\phi n^{39}$$
$$\frac{\partial n^{41}}{\partial t} = \sigma_\gamma^{40}\phi n^{40} - (\lambda^{41} + \sigma_a^{41}\phi)n^{41}$$
$$\frac{\partial n^{42}}{\partial t} = \sigma_\gamma^{41}\phi n^{41} - \sigma_a^{42}\phi n^{42}$$
$$\frac{\partial n^{43}}{\partial t} = \sigma_\gamma^{42}\phi n^{42} - (\lambda^{43} + \sigma_a^{43}\phi)n^{43}$$
$$\frac{\partial n^{51}}{\partial t} = \lambda^{41} n^{41} - (\lambda^{51} + \sigma_a^{51}\phi)n^{51}$$
$$\frac{\partial n^{52}}{\partial t} = \sigma_\gamma^{51}\phi n^{51} - \sigma_a^{52}\phi n^{52}$$
$$\frac{\partial n^{53}}{\partial t} = \lambda^{43} n^{43} - \sigma_a^{53}\phi n^{53} + \sigma_\gamma^{52}\phi n^{52}$$

With respect to Fig. 6.1, a few approximations have been made in writing Eqs. (6.1). The neutron capture in ^{239}U to produce ^{240}U followed by the decay ($t_{1/2} = 14$ h) into ^{240}Np and the subsequent decay ($t_{1/2} = 7$ min) into ^{240}Pu is treated as the direct production of ^{240}Pu by neutron capture in ^{239}U, and the production of ^{240}Np by neutron capture in ^{239}Np followed by the subsequent decay ($t_{1/2} = 7$ min) of ^{240}Np into ^{240}Pu is treated as the direct production of ^{240}Pu by neutron capture in ^{239}Np. These approximations have the beneficial effect for numerical solution techniques of removing short time scales from the set of equations, without sacrificing information of interest on the longer time scale of fuel burnup.

For reactors operating on the thorium cycle, the isotopic concentrations are described by

$$\frac{\partial n^{02}}{\partial t} = -\sigma_a^{02}\phi\, n^{02}$$
$$\frac{\partial n^{03}}{\partial t} = \sigma_\gamma^{02}\phi\, n^{02} - (\lambda^{03} + \sigma_a^{03}\phi)n^{03}$$
$$\frac{\partial n^{13}}{\partial t} = \lambda^{03} n^{03} - (\lambda^{13} + \sigma_a^{13}\phi)n^{13}$$
$$\frac{\partial n^{22}}{\partial t} = -(\lambda^{22} + \sigma_a^{22}\phi)\, n^{22}$$
$$\frac{\partial n^{23}}{\partial t} = \sigma_\gamma^{22}\phi\, n^{22} + \lambda^{13} n^{13} - \sigma_a^{25}\phi\, n^{23} \qquad (6.2)$$
$$\frac{\partial n^{24}}{\partial t} = \sigma_\gamma^{23}\phi\, n^{23} + \sigma_\gamma^{13}\phi\, n^{13} - \sigma_a^{24}\phi\, n^{24}$$
$$\frac{\partial n^{25}}{\partial t} = \sigma_\gamma^{24}\phi\, n^{24} - \sigma_a^{25}\phi\, n^{25}$$

$$\frac{\partial n^{26}}{\partial t} = \sigma_\gamma^{25}\phi\, n^{25} - \sigma_a^{26}\phi\, n^{26}$$
$$\frac{\partial n^{27}}{\partial t} = \sigma_\gamma^{26}\phi\, n^{26} - (\lambda^{27} + \sigma_a^{27}\phi)n^{27}$$
$$\frac{\partial n^{37}}{\partial t} = \lambda^{27} n^{27} - \sigma_a^{37}\phi\, n^{37}$$

Another short-time-scale elimination approximation that neutron capture in ^{233}Pa leads directly to ^{234}U has been made.

Example 6.1: Depletion of a Pure ^{235}U-Fueled Reactor. As an example of the nature of the solution of the equations above, consider the hypothetical case of a reactor initially fueled with pure ^{235}U which operates for 1 year with a constant neutron flux of 10^{14} n/cm^2·s. The solution of the second of Eqs. (6.1) is $n^{25}(t) = n^{25}(0)\ \exp(-\sigma_a^{25}\phi t)$, where at the end of 1 year, $\sigma_a^{25}\phi t = (594 \times 10^{-24}\,\text{cm}^2)(1 \times 10^{14}/\text{cm}^2\text{·s})(3.15 \times 10^7\,\text{s}) = 1.87$ and $n^{25}(t) = 0.154 n^{25}(0)$. The number of atoms that have fissioned in this 1 year is $(n(1) - n(0)) \times [\sigma_f/(\sigma_f + \sigma_\gamma)] = [0.846 n^{25}(0)](507/594) = 0.722 n^{25}(0)$. Each fission event releases 192.9 MeV of recoverable energy, so the total recoverable fission energy release is $[0.722 n^{25}(0)\text{fissions}] \times (192.9\,\text{MeV/fission}) \times (1.6 \times 10^{-19}\,\text{MJ/MeV}) = 2.23 \times 10^{-17} \times n^{25}(0)$ MJ. If the initial core loading is 100 kg of ^{235}U, this corresponds to $(2.23 \times 10^{-17}) \times (10^5/235) \times (6.02 \times 10^{23}) = 0.95 \times 10^9$ MJ $= 1.1 \times 10^4$ MWd of recoverable fission energy.

Neglecting the production of ^{236}U by electron capture decay of ^{236}Np, the solution for $n^{25}(t)$ can be used to solve the third of Eqs. (6.1) to obtain $n^{26}(t) = [n^{25}(0)\ \sigma_\gamma^{25}/(\sigma_a^{25} - \sigma_a^{26})][\exp(-\sigma_a^{26}\phi t) - \exp(-\sigma_a^{25}\phi t)]$. This expression for $n^{26}(t)$ can be used in the fourth of Eqs. (6.1) to obtain a similar, but more complicated solution for $n^{27}(t)$, since we have assumed that $n^{28} = 0$, and so on.

Fission Products

The fission event usually produces two intermediate mass nuclei, in addition to releasing two or three neutrons. Interestingly, the fission product masses are not usually equal to about half the mass of the fissioning species, but are distributed in mass with peaks at about 100 and 140 amu, as shown in Fig. 6.2. The isotopes produced by fission tend to be neutron-rich and undergo radioactive decay. They also undergo neutron capture, with cross sections ranging from a few tenths of a barn to millions of barns. The general production–destruction equation satisfied by a fission product species j is

$$\frac{dn_j}{dt} = \gamma_j \Sigma_f \phi + \sum_i (\lambda^{i\to j} + \sigma^{i\to j}\phi) n_i - (\lambda^j + \sigma_a^j \phi) n_j \qquad (6.3)$$

where γ_j is the fraction of

Where γ_j is the fraction of fission events that produce a fission product species j. $\lambda^{i\to j}$ is the decay rate of isotope i to produce isotope j. (β, α, n, etc.

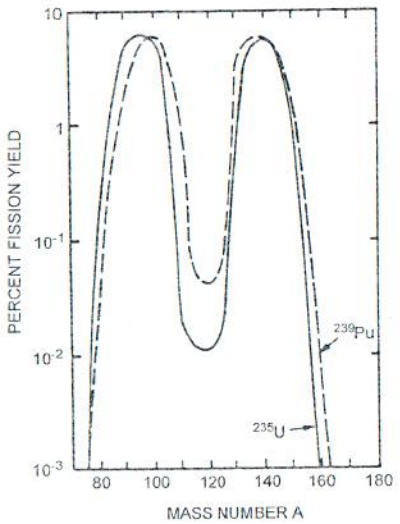

Fig. 6.2 Fission yields for ^{235}U and ^{239}Pu. (From Ref. 15.)

decay) and $\sigma^{i\to j}$ is the transmutation cross section for the production of isotope j by neutron capture in isotope j. Even though the fission products undergo transmutation and decay, the total inventory of direct fission products plus their progeny increases in time as

$$\frac{dn_{fp}}{dt} = \sum_j \frac{dn_j}{dt} = \sum_j \gamma_j \Sigma_f \phi \tag{6.4}$$

Solution of the Depletion Equations

The equations above can be integrated to determine composition changes over the lifetime of the reactor core loading if the time dependence of the flux is known. However, the flux distribution depends on the composition. In practice, a neutron flux distribution is calculated for the beginning-of-cycle composition and critical control rod position or soluble boron concentration (PWR), and this flux distribution is used to integrate the composition equations above over a depletion-time step, Δt_{burn}. Then the new critical control rod position or soluble boron concentration is determined (by trial and error) and the flux distribution is recalculated for use in integrating the production–destruction equations over the next depletion time step,

and so on, until end-of-cycle is reached. The maximum value of Δt_{burn} depends

on how fast the composition is changing and the effect of that composition change on the neutron flux distribution and on the accuracy of the numerical integration scheme. Excluding, for the moment, the relatively short time scale phenomena associated with the xenon and samarium fission products, the time scale of significant composition and flux changes is typically several hundred hours or more.

The typical process of advancing the depletion solution from time t_i, at which the composition is known, to time t_{i+1} is: (1) determine the multigroup constants appropriate for the composition at t_i, (2) determine the critical control rod positions or soluble poison concentration by solving the multigroup diffusion equations for the flux at t_i (adjusting the control rod positions or boron concentration until the reactor is critical), and (3) integrate the various fuel and fission product production–destruction equations from t_i to t_{i+1}. (The neutron flux solution could be made with a multigroup transport calculation or with multigroup or continuous-energy Monte Carlo calculation, and the preparation of cross sections could involve infinite media spectra and unit cell homogenization calculations or could be based on fitted, precomputed constants.) The integration of the production–destruction equations can be for a large number of points, using the neutron flux at each point; for each fuel pin, using the average flux in the fuel pin; for each fuel assembly, using the average flux over the fuel assembly; and so on.

Assuming that the flux is constant in the interval $t_i < t < t_{i+1}$, the production–destruction equations can be written in matrix notation as

$$\frac{d\boldsymbol{N}(t)}{dt} = \boldsymbol{A}(\phi(t_i))\boldsymbol{N}(t) + \boldsymbol{F}(\phi(t_i)), \qquad t_i \le t \le t_{i+1} \tag{6.5}$$

The general solution to these equations is of the form

$$N(t_{i+1}) = \exp[\boldsymbol{A}(t_i)\Delta t]\boldsymbol{N}(t_i) + \boldsymbol{A}^{-1}(t_i)\{\exp[\boldsymbol{A}(t_i)\Delta t] - 1\}F(t_i) \tag{6.6}$$

In general, the accuracy of the solution depends on Δt_{burn} being chosen so that $(\lambda^i + \sigma_a^i \varphi)\Delta t_{\text{burn}} \ll 1$ for all of the isotopes involved. For this reason, it is economical to reformulate the physical production–destruction equations to eliminate short-time-scale phenomena that do not aect the overall result, as discussed previously. There exist a number of computer codes that solve the production–destruction equations for input neutron fluxes (e.g., Ref. 7).

Measure of Fuel Burnup

The most commonly used measure of fuel burnup is the fission energy release per unit mass of fuel. The fission energy release in megawatt-days divided by the total mass (in units of 1000 kg or 1 tonne) of fuel nuclei (fissile plus fertile) in the initial loading is referred to as *megawatt-days per tonne* (MWd/T). An equivalent unit is MWd/kg—10^3 MWd/T. For example, a reactor with 100,000 kg of fuel operating at 3000 MW power level for 1000 days would have a burnup of 30,000 MWd/T

For LWRs the typical fuel burnup is 30,000 to 50,000 MWd/T. Fuel burnup in fast reactors is projected up to be about 100,000 to 150,000 MWd/T.

Fuel Composition Changes with Burnup

The original fissionable isotope (e.g., ^{235}U) naturally decreases as the reactor operates. However, the neutron transmutation of the fertile isotope (e.g., ^{238}U) produces the fissionable isotope ^{239}Pu, which in turn is transmuted by neutron capture into ^{240}Pu and higher actinide isotopes. The buildup of the various Pu isotopes as a function of fuel burnup for a typical LWR is shown in Fig. 6.3.

Compositions of spent fuel discharged from representative LWR and LMFBR designs are given in Table 6.2. The units are densities (cgs units) times 10^{-24}, which allows construction of macroscopic cross section upon multiplication by the microscopic cross section in barns. The composition for the average enrichment and burnup of PWR spent fuel is shown in the first column for fuel discharged before 1995 and in the second column for fuel discharged after 1995.

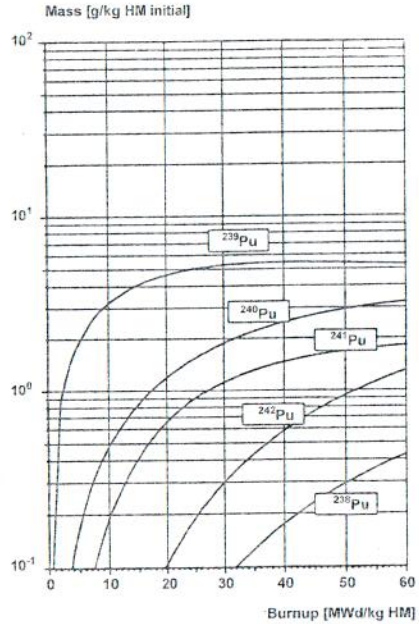

Fig. 6.3 Buildup of Pu isotopes in 4 wt % enriched UO_2 in an LWR. (From Ref. 1; used

TABLE 6.2 Heavy Metal Composition of Spent UO_2 Fuel at Discharge[a]

Reactor Type	LWR	LWR	LMFBR	LMFBR
Initial enrichment (wt %)	3.13	4.11	20	20
Power (MW/MTU)	21.90	27.99	54.76	54.76
Burnup (GWd/T)	32	46	100	150
Actinides (1×10^{24} cm^{-3})				
^{234}U	3.92×10^{-6}	4.51×10^{-6}	3.37×10^{-5}	2.88×10^{-5}
^{235}U	1.92×10^{-4}	1.72×10^{-4}	2.17×10^{-3}	1.37×10^{-3}
^{236}U	8.73×10^{-5}	1.23×10^{-4}	4.58×10^{-4}	5.62×10^{-4}
^{237}U	[b]	2.48×10^{-7}	5.71×10^{-7}	7.89×10^{-7}
^{238}U	2.12×10^{-2}	2.08×10^{-2}	1.63×10^{-2}	1.53×10^{-2}
^{237}NP	1.01×10^{-5}	1.64×10^{-5}	5.11×10^{-5}	1.01×10^{-4}
^{239}NP	1.25×10^{-6}	1.55×10^{-6}	2.93×10^{-6}	3.16×10^{-6}
^{238}PU	3.36×10^{-6}	6.56×10^{-6}	3.84×10^{-6}	1.20×10^{-5}
^{239}PU	1.23×10^{-4}	1.23×10^{-4}	1.04×10^{-3}	1.36×10^{-3}
^{240}PU	4.05×10^{-5}	4.28×10^{-5}	7.83×10^{-5}	1.71×10^{-4}
^{241}PU	3.44×10^{-5}	4.07×10^{-5}	2.60×10^{-6}	8.37×10^{-6}
^{242}PU	1.05×10^{-5}	1.69×10^{-5}	[b]	4.70×10^{-7}
^{241}AM	1.45×10^{-6}	1.62×10^{-6}	1.50×10^{-7}	6.87×10^{-7}
^{243}AM	2.12×10^{-6}	4.46×10^{-6}	[b]	[b]
^{242}CM	3.71×10^{-7}	5.66×10^{-7}	[b]	[b]
^{244}CM	4.81×10^{-7}	1.39×10^{-6}	[b]	[b]

[a]Calculated with ORIGEN (Ref. 7).

[b]$< 0.001\%$.

Reactivity Effects of Fuel Composition Changes

There are a variety of reactivity effects associated with the change in fuel composition. The fission of fuel nuclei produces two negative reactivity effects; the number of fuel nuclei is reduced and fission products are created, many of which have large neutron capture cross sections. The transmutation–decay chain of fertile fuel nuclei of a given species produces a sequence of actinides (uranium-fueled reactor) or uranium isotopes (thorium-fueled reactor), some of which are fissile. The transmutation of one fertile isotope into another nonfissile isotope can have a positive or negative reactivity effect, depending on the cross sections for the isotopes involved, but the transmutation of a fertile isotope into a fissile isotope has a positive reactivity effect. Depending on the initial enrichment, the transmutation–decay process generally produces more fissile nuclei than are destroyed early in the cycle, causing a positive reactivity effect, until the concentration of transmuted fissile nuclei comes into equilibrium.

The buildup of ^{239}Pu early in life of a uranium-fueled reactor produces a large positive reactivity effect which may be greater than the negative reactivity effect of ^{235}U depletion and fission product buildup. For thermal reactors, $\eta^{40} < \eta^{25}$, so the buildup of ^{239}Pu must exceed the burnup of ^{235}U in order for a positive reactivity

effect. For fast reactors, $\eta^{49} > \eta^{25}$ for neutron energies in excess of about 10 keV, and there can be an initial positive reactivity effect even if the decrease in ^{235}U is greater than the buildup of ^{239}Pu. However, the ^{239}Pu concentration will saturate at a value determined by the balance between the ^{238}U transmutation rate and the ^{239}Pu depletion rate, at which point the continued depletion of ^{235}U and buildup of fission products produce a negative reactivity effect that accrues over the lifetime of the fuel in the reactor.

Compensating for Fuel-Depletion Reactivity Effects

The reactivity effects of fuel depletion must be compensated to maintain criticality over the fuel burnup cycle. The major compensating elements are the control rods, which can be inserted to compensate positive depletion reactivity effects and withdrawn to compensate negative depletion reactivity effects. Adjustment of the concentration of a neutron absorber (e.g., boron in the form of boric acid) in the water coolant is another means used to compensate for fuel-depletion reactivity effects. *Soluble poisons* are used to compensate fuel-depletion reactivity in PWRs but not in BWRs, because of the possibility that they will plate out on boiling surfaces. Since a soluble poison introduces a positive coolant temperature reactivity coefficient because an increase in temperature decreases the density of the soluble neutron absorber, the maximum concentration (hence the amount of fuel depletion reactivity that can be compensated) is limited.

Burnable poisons (e.g., boron, erbium, or gadolinium elements located in the fuel lattice), which themselves deplete over time, can be used to compensate the negative reactivity effects of fuel depletion. The concentration of burnable poison can be described by

$$\frac{dn^{bp}}{dt} = -f_{bp} n^{bp} \sigma_{bp} \phi \tag{6.7}$$

where f_{bp} is the self-shielding of the poison element (i.e., the ratio of the neutron flux in the poison element to the neutron flux in the adjacent fuel assembly). The poison concentration is chosen so that the spatial self-shielding of the poison elements is large enough ($f_{bp} \ll 1$) early in the burnup cycle to shield the poison from neutron capture, and the neutron capture rate remains constant in time. After a certain time the concentration of the poison nuclei is sufficiently reduced that f_{bp} increases and the poison burns out, resulting in an increasing reactivity. If the poison starts to burn out at about the same time that the overall fuel depletion reactivity effect starts to become progressively more negative (i.e., when the ^{239}Pu concentration saturates), the burnout of the poison will at least partially compensate the fuel-depletion reactivity decrease.

Reactivity Penalty

While ^{239}Pu and ^{241}Pu are fissionable in a thermal reactor, and ^{240}Pu transmutes into ^{241}Pu, ^{242}Pu transmutes into ^{243}Pu with a rather small cross section, and ^{243}Pu has a rather small fission cross section, so that ^{242}Pu is effectively a parasitic absorber that builds up in time. The ^{243}Am also accumulates and acts primarily as a parasitic absorber. Whereas the ^{243}Am, which is produced by the decay of ^{243}Pu, can be separated readily, it is difficult to separate the different plutonium isotopes from each other, so the negative ^{242}Pu reactivity effect is exacerbated if the plutonium is recycled with uranium. A similar problem arises with the ^{236}U produced by radiative capture in ^{235}U, as shown in Fig. 6.4, which is difficult to separate from ^{235}U, and with ^{237}Np, which is produced by transmutation of ^{236}U into ^{237}U followed by beta decay. The ^{237}Np can be separated readily, however, and does not need to accumulate in recycled fuel.

End-of-cycle reactivity penalties calculated for the recycle of BWR fuel are shown in Table 6.3 after one, two, and three cycles. It was assumed that the ^{237}Np and ^{243}Am were removed between cycles, but there was a cycle-to-cycle increase in the ^{237}Np and ^{243}Am reactivity penalties due to the accumulation of ^{236}U and ^{242}Pu, respectively.

Effects of Fuel Depletion on the Power Distribution

Fuel depletion and the compensating control actions affect the reactor power distribution over the lifetime of the fuel in the core. Depletion of fuel will be greatest where the power is greatest. The initial positive reactivity effect of depletion will then enhance the power peaking. At later times, the negative reactivity effects will cause the power to shift away to regions with higher $k_{infinity}$. Any strong tendency of

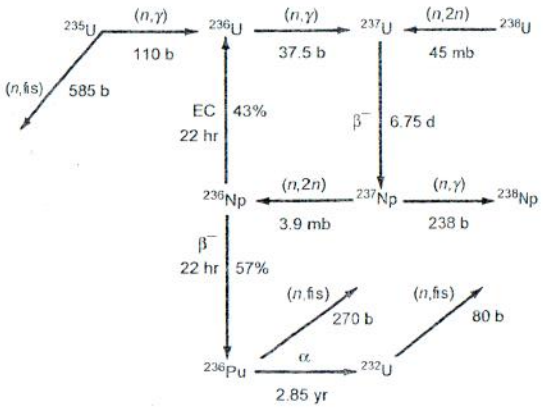

Fig 6.4

TABLE 6.3 Reactivity Penalties with Recycled BWR Fuel (% $\Delta k/k$)

End of Cycle:	^{236}U	^{237}Np	^{242}Pu	^{243}Am
1	0.62	0.13	0.65	0.36
2	0.90	0.59	1.53	0.57
3	1.12	0.73	2.04	0.89

Source: Data from Ref. 16.

the power distribution to peak as a result of fuel depletion must be compensated by control rod movement. However, the control rod movement to offset fuel depletion reactivity effects itself produces power peaking; the presence of the rods shields the nearby fuel from depletion and when the rods are withdrawn, the higher local k_∞ causes power peaking. Similarly, burnable poisons shield the nearby fuel, producing local regions of higher k_∞ and power peaking when they burn out. Determination of the proper fuel concentration zoning and distribution of burnable poisons and of the proper control rod motion to compensate fuel depletion reactivity effects without unduly large power peaking is a major nuclear analysis task.

In-Core Fuel Management

At any given time, the fuel in a reactor core will consist of several batches that have been in the core for different lengths of time. The choice of the number of batches is made on the basis of a trade-off between maximizing fuel burnup and minimizing the number of shutdowns for refueling, which reduces the plant capacity factor. At each refueling, the batch of fuel with the highest burnup is discharged, the batches with lower burnup may be moved to different locations, and a fresh or partially depleted batch is added to replace the discharged batch. The analysis leading to determination of the distribution of the fuel batches within the core to meet the safety, power distribution and burnup, or cycle length constraints for fuel burn cycle is known as *fuel management analysis*. Although fuel management may be planned in advance, it must be updated online to adjust to higher or lower capacity factors than planned (which result in lower or higher reactivity than planned at the planned refueling time) and unforeseen outages (which result in higher reactivity than planned at the planned refueling time).

Typically, a PWR will have three fuel batches, and a BWR will have four fuel batches in the core at any given time and will refuel every 12 to 18 months. A number of different loading patterns have been considered, with the general conclusion that more energy is extracted from the fuel when the power distribution in the core is as flat as possible. In the *in–out loading pattern*, the reactor is divided into concentric annular regions loaded with different fuel batches. The fresh fuel batch is placed at the periphery, the highest burnup batch is placed at the center, and intermediate burnup batches are placed in between to counter the natural tendency of power to peak in the center of the core. At refueling, the central batch is

discharged, the other batches are shifted inward, and a fresh batch is loaded on the periphery. The in–out loading pattern has been found to go too far in the sense that the power distribution is depressed in the center and peaked at the periphery. An additional difficulty is the production of a large number of fast neutrons at the periphery that leak from the core and damage the pressure vessel.

In the *scatter loading pattern* the reactor core is divided into many small regions of four to six assemblies from different batches. At refueling, the assemblies within each region with the highest burnup are discharged and replaced by fresh fuel assemblies. This loading pattern has been found to produce a more uniform power distribution and to result in less fast neutron leakage than the in–out pattern.

Since the pressure vessel damage by fast neutrons became recognized as a significant problem, a number of different loading patterns have been developed with the specific objective of minimizing neutron damage to the pressure vessel. These include placement of only partially depleted assemblies at the core periphery, placement of highly depleted assemblies near welds and other critical locations, using burnable poisons in peripheral assemblies, replacing peripheral fuel assemblies with dummy assemblies, and others.

Better utilization of resources argues for the highest possible fuel burnup consistent with materials damage limitations, and a new higher enrichment fuel has been developed that can achieve burnups of up to 50,000 MWd/T in LWRs. The higher fuel burnup produces more actinides and fission products with large thermal neutron cross sections, which compete more effectively with control rods for thermal neutrons and reduces control rod worth, and which produces larger coolant temperature reactivity coefficients. The higher-enrichment higher-burnup fuel also provides the possibility of longer refueling cycles, which improves plant capacity factor and reduces power costs.

6.2 SAMARIUM AND XENON

The short-term time dependence of two fission product progeny, ^{149}Sm and ^{135}Xe, which have very large absorption cross sections, introduces some interesting reactivity transients when the reactor power level is changed.

Samarium Poisoning

Samarium-149 is produced by the beta decay of the fission product ^{149}Nd, as described in Fig. 6.5. It has a thermal neutron absorption cross section of 4×10^4 barns and a large epithermal absorption resonance. The 1.7-h half-life of ^{149}Nd is sufficiently short that ^{149}Pm can be assumed to be formed directly from fission in writing the production–destruction equations for ^{149}Sm:

$$\frac{dP}{dt} = \gamma^{Nd}\Sigma_f\phi - \lambda^P P$$
$$\frac{dS}{dt} = \lambda^P P - \sigma_a^S \phi S \tag{6.8}$$

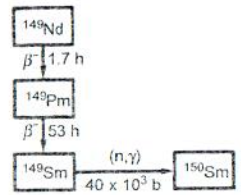

(a)

FISSILE NUCLIDE	γ^{Nd}
^{233}U	0.0066
^{235}U	0.0113
^{239}Pu	0.0190

(b)

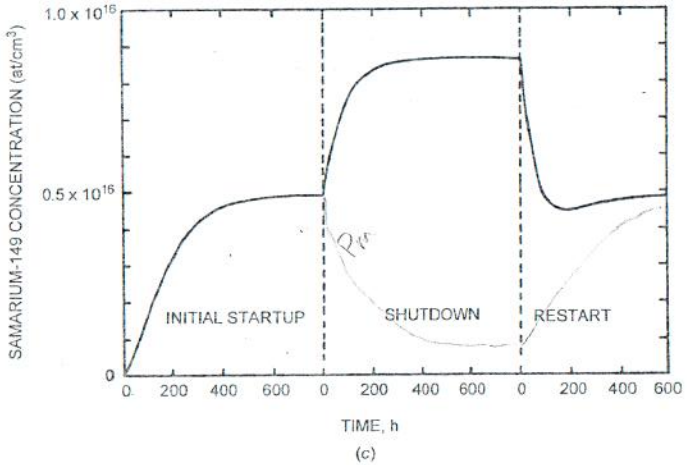

(c)

Fig. 6.5 Characteristics of ^{149}Sm under representative LWR conditions: (*a*) transmutation–decay chain; (*b*) fission yields; (*c*) time dependence. (From Ref. 3; used with permission of Taylor & Francis/Hemisphere Publishing.)

where P and S refer to ^{149}Pm and ^{149}Sm, respectively. These equations have the solution, for constant ϕ,

$$P(t) = \frac{\gamma^{Nd}\Sigma_f\phi}{\lambda^P}(1 - e^{-\lambda^P t}) + P(0)e^{-\lambda^P t}$$

$$S(t) = S(0)e^{-\sigma_a^S\phi t} + \frac{\gamma^{Nd}\Sigma_f}{\sigma_a^S}(1 - e^{-\sigma_a^S\phi t}) \qquad (6.9)$$

$$- \frac{\gamma^{Nd}\Sigma_f\phi - \lambda^P P(0)}{\lambda^P - \sigma_a^S\phi}(e^{-\sigma_a^S\phi t} - e^{-\lambda^P t})$$

At the beginning of life in a fresh core, $P(0) = S(0) = 0$, and the promethium and samarium concentrations build up to equilibrium values:

$$P_{eq} = \frac{\gamma^{Nd}\Sigma_f\phi}{\lambda^P}, \qquad S_{eq} = \frac{\gamma^{Nd}\Sigma_f}{\sigma_a^S} \qquad (6.10)$$

The equilibrium value of ^{149}Pm depends on the neutron flux level. However, the equilibrium value of ^{149}Sm is determined by a balance between the fission production rate of ^{149}Pm and the neutron transmutation rate of ^{149}Sm, both of which are proportional to the neutron flux, and consequently, does not depend on the neutron flux level. The time required for the achievement of equilibrium concentrations depends on ϕ, σ_a^S and λ^P. For typical thermal reactor flux levels (e.g., 5×10^{13} n/cm^2·s), equilibrium levels are achieved in a few hundred hours.

When a reactor is shut down after running sufficiently long to build up equilibrium concentrations, the solutions of Eqs. (6.9) with $P(0) = P_{eq}$, $S(0) = S_{eq}$, and $\phi = 0$ are

$$P(t) = P_{eq}e^{-\lambda^P t}$$

$$S(t) = S_{eq} + P_{eq}(1 - e^{-\lambda^P t}) \rightarrow S_{eq} + P_{eq} \qquad (6.11)$$

indicating that the ^{149}Sm concentration will increase to $S_{eq} + P_{eq}$ as the ^{149}Pm decays into ^{149}Sm with time constant $1/\lambda^P = 78$ h. If the reactor is restarted, the ^{149}Sm burns out until the ^{149}Pm builds up; then the ^{149}Sm returns to its equilibrium value. This time dependence of the samarium concentration is illustrated in Fig. 6.5.

The perturbation theory estimate for the reactivity worth of ^{149}Sm is

$$\rho_{Sm}^{(t)} = -\frac{S(t)\sigma_a^S}{\Sigma_a} \qquad (6.12)$$

which for the equilibrium concentration becomes

$$\rho_{Sm}^{eq} = -\frac{\gamma^{Nd}\Sigma_f}{\sigma_a^S}\frac{\sigma_a^S}{\Sigma_a} = -\gamma^{Nd}\frac{\Sigma_f}{\Sigma_a} = -\frac{\gamma^{Nd}}{\nu} \qquad (6.13)$$

where we have used the approximation that $k \approx \nu\Sigma_f/\Sigma_a = 1$. For a ^{235}U-fueled reactor, $\rho_{Sm}^{eq} \approx 0.0045$.

Xenon Poisoning

Xenon-135 has a thermal absorption cross section of 2.6×10^6 barns. It is produced directly from fission, with yield γ^{Xe}, and from the decay of ^{135}I, which in turn is produced by the decay of the direct fission product ^{135}Te, with yield γ^{Te}, as indicated in Fig. 6.6. The production–destruction equations may be written, with the

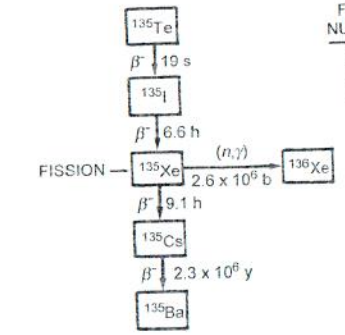

(a)

FISSILE NUCLIDE	$\gamma^{(135}$Te)	$\gamma^{(135}$Xe)
^{233}U	0.051	0.003
^{235}U	0.061	
^{239}Pu	0.055	

(b)

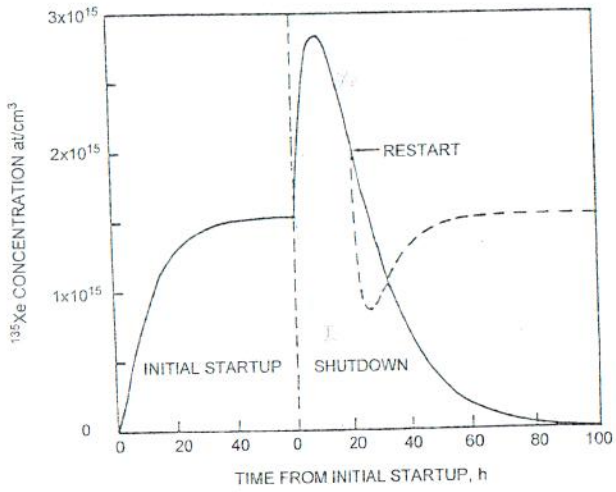

(c)

Fig. 6.6 Characteristics of ^{135}Xe under representative LWR conditions: (*a*) transmutation–decay chain; (*b*) fission yields; (*c*) time dependence. (From Ref. 3; used with permission of Taylor & Francis/Hemisphere Publishing.)

assumption that ^{135}I is produced directly from fission with yield γ^{Te},

$$\begin{aligned}\frac{dI(t)}{dt} &= \gamma^{\mathrm{Te}}\Sigma_f\phi - \lambda^I I \\ \frac{dX(t)}{dt} &= \gamma^{\mathrm{Xe}}\Sigma_f\phi + \lambda^I I - (\lambda^X + \sigma_a^X\phi)X\end{aligned} \tag{6.14}$$

These equations have the solutions

$$\begin{aligned}I(t) &= \frac{\gamma^{\mathrm{Te}}\Sigma_f\phi}{\lambda^I}(1 - e^{-\lambda^I t}) + I(0)e^{-\lambda^I t} \\ X(t) &= \frac{(\gamma^{\mathrm{Te}} + \gamma^{\mathrm{Xe}})\Sigma_f\phi}{\lambda^X + \sigma_a^X\phi}[1 - e^{-(\lambda^X + \sigma_a^X\phi)t}] \\ &\quad + \frac{\gamma^{\mathrm{Te}}\Sigma_f\phi - \lambda^I I(0)}{\lambda^X - \lambda^I + \sigma_a^X\phi}[e^{-(\lambda^X + \sigma_a^X\phi)t} - e^{-\lambda^I t}] + X(0)e^{-(\lambda^X + \sigma_a^X\phi)t}\end{aligned} \tag{6.15}$$

When the reactor is started up from a clean condition in which $X(0) = I(0) = 0$, or the reactor power level is changed, the ^{135}I and ^{135}Xe concentrations approach equilibrium values:

$$I_{\mathrm{eq}} = \frac{\gamma^{\mathrm{Te}}\Sigma_f\phi}{\lambda^I}, \qquad X_{\mathrm{eq}} = \frac{(\gamma^{\mathrm{Te}} + \gamma^{\mathrm{Xe}})\Sigma_f\phi}{\lambda^X + \sigma_a^X\phi} \tag{6.16}$$

with time constants $1/\lambda^I = 0.1$ h and $1/(\lambda^X + \sigma_a^X\varphi) \approx 30$ h, respectively. The perturbation theory estimate of the reactivity worth of equilibrium xenon is

$$\rho_{\mathrm{Xe}}^{\mathrm{eq}} = -\frac{\sigma_a^X(\gamma^{\mathrm{Te}} + \gamma^{\mathrm{Xe}})\Sigma_f\phi}{\Sigma_a(\lambda^X + \sigma_a^X\phi)} \simeq -\frac{\gamma^{\mathrm{Te}} + \gamma^{\mathrm{Xe}}}{\nu(1 + \lambda^X/\sigma_a^X\phi)} = \frac{0.026}{1 + (0.756 \times 10^{13})/\phi} \tag{6.17}$$

Peak Xenon

When a reactor is shut down from an equilibrium xenon condition, the iodine and xenon populations satisfy Eqs. (6.15) with $I(0) = I_{\mathrm{eq}}$, $X(0) = X_{\mathrm{eq}}$, and $\phi = 0$:

$$\begin{aligned}I(t) &= I_{\mathrm{eq}}e^{-\lambda^I t} \\ X(t) &= X_{\mathrm{eq}}e^{-\lambda^X t} + I_{\mathrm{eq}}\frac{\lambda^I}{\lambda^I - \lambda^X}(e^{-\lambda^X t} - e^{-\lambda^I t})\end{aligned} \tag{6.18}$$

If $\phi > (\gamma^X/\gamma^{\mathrm{Te}})(\lambda^X/\sigma_a^X)$, the xenon will build up after shutdown to a peak value at time

$$t_{\mathrm{pk}} = \frac{1}{\lambda^I - \lambda^X}\ln\frac{\lambda^I/\lambda^X}{1 + (\lambda^X/\lambda^I)(\lambda^I/\lambda^X - 1)(X_{\mathrm{eq}}/I_{\mathrm{eq}})} \tag{6.19}$$

and then decay to zero unless the reactor is restarted. For ^{235}U- and ^{233}U-fueled reactors $\phi > 4 \times 10^{11}$ and 3×10^{12} n/cm^2·s, respectively, is sufficient for an increase in the xenon concentration following shutdown. Typical flux values (e.g., 5×10^{13} n/cm^2·s) in thermal reactors are well above these threshold levels, and for typical flux values, Eq. (6.19) yields a peak xenon time of ≈ 11.6 h. If the reactor is restarted before the xenon has entirely decayed, the xenon concentration will initially decrease because of the burnout of xenon and then gradually build up again because of the decay of a growing iodine concentration, returning to values of I_{eq} and X_{eq} for the new power level. This time dependence of the xenon concentration is illustrated in Fig. 6.6.

Effect of Power-Level Changes

When the power level changes in a reactor (e.g., in load following) the xenon concentration will change. Consider a reactor operating at equilibrium iodine $I_{eq}(\phi_0)$ and xenon $X_{eq}(\phi_0)$ at flux level ϕ_0. At $t = t_0$ the flux changes from ϕ_0 to ϕ_1. Equations (6.16) can be written

$$I(t) = I_{eq}(\phi_1)\left(1 - \frac{\phi_1 - \phi_0}{\phi_1} e^{-\lambda^I t}\right)$$

$$X(t) = X_{eq}(\phi_1)\left(1 - \frac{\phi_1 - \phi_0}{\phi_1}\left\{\frac{\lambda^X}{\lambda^X + \sigma_a^X \phi_a} e^{-(\lambda^X + \sigma_a^X \phi_1)t} + \frac{\gamma^{Te}}{\gamma^{Te} + \gamma^{Xe}} \frac{\lambda^X + \sigma_a^X \phi_1}{\lambda^X - \lambda^I + \sigma_a^X \phi_1}\left[e^{-\lambda^I t} - e^{-(\lambda^X + \sigma_a^X \phi_1)}\right]\right\}\right) \tag{6.20}$$

The xenon concentration during a transient of this type is shown in Fig. 6.7.

The perturbation theory estimate for the reactivity worth of xenon at any time during the transient discussed above is

$$\rho_{Xe}(t) = -\frac{\sigma_a^X X(t)}{\Sigma_a} \simeq -\frac{\sigma_a^X X(t)}{\nu \Sigma_f} \tag{6.21}$$

Example 6.2: Xenon Reactivity Worth. As an example of xenon buildup, consider a ^{235}U-fueled reactor that has operated at a thermal flux level of 5×10^{13} cm^{-2} s^{-1} for two months such that equilibrium xenon and iodine have built in to the levels given by Eqs. (6.16). Using $\sigma_a^X = 2.6 \times 10^{-18}$ cm^2, $t_{1/2}^I = 6.6$ h, $t_{1/2}^X = 9.1$ h, $\lambda = \ln 2/t_{1/2}$, $\gamma_{Te} = 0.061$, and $\gamma_{Xe} = 0.003$, the equilibrium values of xenon and iodine are $X^{eq} = 0.0203 \times 10^{18}\ \Sigma_f$ cm^{-3} and $I^{eq} = 0.1051 \times 10^{18}\ \Sigma_f$ cm^{-3}. The reactivity worth of equilibrium xenon is $\rho_{Xe}^{eq} \approx \sigma_a^X X^{eq}/\Sigma_a \approx 0.022\,\Delta k/k$, where the approximate criticality condition $\nu\Sigma_f \approx \Sigma_a$ has been used.

If the reactor is shut down for 6 h and then restarted, the xenon reactivity worth that must be compensated is, from Eqs. (6.16) and (6.21), $\rho_{Xe}(t = 6\text{ h}) \approx \sigma_a^X X(t = 6\text{ h})/\nu\Sigma_f = (0.634X^{eq} + 0.367I^{eq}) \times \sigma^X/\nu\Sigma_f = 0.0171 + 0.04 = 0.0571\,\Delta k/k$

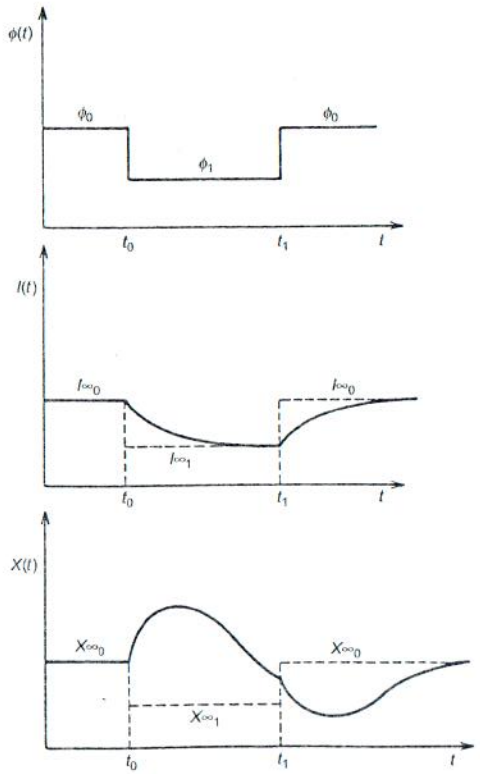

Fig. 6.7 Xenon concentration following power-level changes. (From Ref. 9; used with permission of Wiley.)

The largest contribution to the xenon worth at 6 h after shutdown clearly comes from buildup of xenon from the decay of the iodine concentration at shutdown at a faster rate than the resulting xenon decays.

6.3 FERTILE-TO-FISSILE CONVERSION AND BREEDING

Availability of Neutrons

The transmutation–decay processes depicted in Fig. 6.1 hold out the potential for increasing the recoverable energy content from the world's uranium and thorium

resources by almost two orders of magnitude by converting the fertile isotopes ^{238}U and ^{232}Th, which only fission at very high neutron energies, into fissile isotopes, ^{239}Pu and ^{241}Pu in the case of ^{238}U, and ^{233}U in the case of ^{232}Th, which have large fission cross sections for thermal neutrons and substantial fission cross sections for

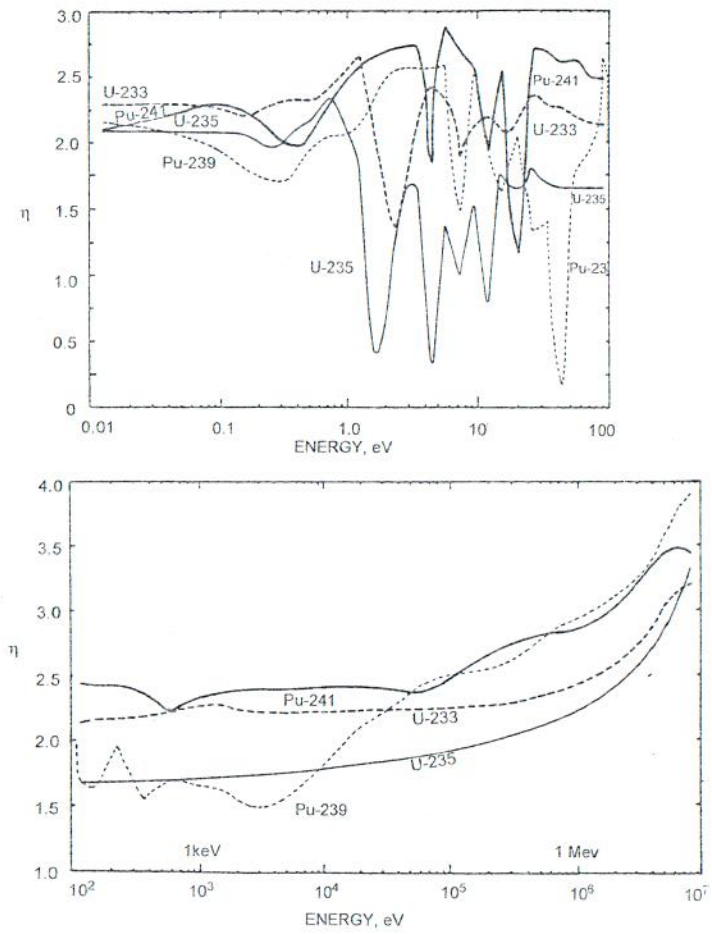

Fig. 6.8 Parameter η for the principal fissile nuclei. (From Ref. 17; used with permission of

fast neutrons. The rate of transmutation of fertile-to-fissile isotopes depends on the number of neutrons in excess of those needed to maintain the chain fission reaction that are available. In the absence of neutron absorption by anything other than fuel and in the absence of leakage, the number of excess neutrons is $\eta - 1$. The quantity η is plotted in Fig. 6.8 for the principal fissile isotopes.

The fertile-to-fissile conversion characteristics depend on the fuel cycle and the neutron energy spectrum. For a thermal neutron spectrum ($E < 1$ eV), ^{233}U has the largest value of η of the fissile nuclei. Thus the best possibility for fertile-to-fissile conversion in a thermal spectrum is with the ^{232}Th–^{233}U fuel cycle. For a fast neutron spectrum ($E > 5 \times 10^4$ eV), ^{239}Pu and ^{241}Pu have the largest values of η of the fissile nuclei. The LMFBR, based on the ^{238}U–^{239}Pu fuel cycle, is intended to take advantage of the increase of η[49] at high neutron energy.

Conversion and Breeding Ratios

The instantaneous *conversion ratio* is defined as the ratio of the rate of creation of new fissile isotopes to the rate of destruction of fissile isotopes. When this ratio is greater than unity, it is conventional to speak of a *breeding ratio*, because the reactor would then be producing more fissile material than it was consuming. Average conversion or breeding ratios calculated for reference reactor designs of various types are shown in Table 6.4.

The values of the conversion ratios for the PWR and BWR are the same because of design similarities. The HTGR conversion ratio is somewhat higher because of the higher value of η for ^{233}U than for ^{235}U. The improved conversion ratio for the CANDU–PHWR is due to the better neutron economy provided by online refueling and consequent reduced requirements for control poisons to compensate excess reactivity.

The breeding ratio in an LMFBR can vary over a rather wide range, depending on the neutron energy spectrum. Achieving a large value of η and hence a large breeding ratio favors a hard neutron spectrum. However, a softer spectrum is favored for safety reasons—the lower-energy neutrons which are subject to resonance absorption become more likely to be radiatively captured than to cause fission as the neutron energy is reduced, as discussed in Chapter 5.

TABLE 6.4 Conversion/Breeding Ratios in Different Reactor Systems

Reactor System	Initial Fuel	Conversion Cycle	Conversion Ratio
BWR	2–4 wt % ^{235}U	^{238}U–^{239}Pu	0.6
PWR	2–4 wt % ^{235}U	^{238}U–^{239}Pu	0.6
PHWR	Natural U	^{238}U–^{239}Pu	0.8
HTGR	≈5 wt % ^{235}U	^{232}Th–^{233}U	0.8
LMFBR	10–20 wt % Pu	^{238}U–^{239}Pu	1.0–1.6

6.4 SIMPLE MODEL OF FUEL DEPLETION

The concepts involved in fuel depletion and the compensating control adjustment can be illustrated by a simple model in which the criticality requirement is written as

$$k = \eta f = \frac{\eta \Sigma_a^F(t)}{\Sigma_a^F(t) + \Sigma_a^M + \Sigma_a^{\text{fp}}(t) + \Sigma_c(t)} = 1 \tag{6.22}$$

where Σ_a^F is the fuel macroscopic absorption cross section, Σ_a^M the moderator macroscopic absorption cross section, and Σ_a^C the combined (soluble and burnable poisons plus control rod) control absorption cross section. Assuming that the reactor operates at constant power $\nu\Sigma_f^F(t)\phi(t) = \nu\Sigma_f^F(0)\phi(0)$ and that $\eta = \nu\Sigma_f^F/\Sigma_a^F$ is constant in time, the fuel macroscopic absorption cross section at any time is

$$\begin{aligned}\Sigma_a^F(t) &= N_F(t)\sigma_a^F = \sigma_a^F\left[N_F(0) - \varepsilon\sigma_a^F\int_0^t N_F(t')\phi(t')dt'\right] \\ &= N_F(0)\sigma_a^F[1 - \varepsilon\phi(0)\sigma_a^F t]\end{aligned} \tag{6.23}$$

The neutron flux is related to the beginning-of-cycle neutron flux by

$$\phi(t) = \frac{\phi(0)}{1 - \varepsilon\sigma_a^F\phi(0)t} \tag{6.24}$$

where $\varepsilon < 1$ is a factor that accounts for the production of new fissionable nuclei via transmutation–decay.

The fission product cross section is the sum of the equilibrium xenon and samarium cross sections constructed using Eqs. (6.16) and (6.10), respectively, and an effective cross section for the other fission products,

$$\Sigma_{\text{fp}'} = \sigma_{\text{fp}'}\gamma_{\text{fp}'}\Sigma_f(t)\phi(t)t = \sigma_{\text{fp}'}\gamma_{\text{fp}'}\Sigma_f(0)\phi(0)t \tag{6.25}$$

which accumulate in time from fission with yield $\gamma_{\text{fp}'}$. The quantity $\gamma_{\text{fp}'}\sigma_{\text{fp}'}$ is about 40 to 50 barns per fission. Using these results, Eq. (6.22) can be solved for the value of the control cross section that is necessary to maintain criticality:

$$\begin{aligned}\Sigma_c(t) = (\eta-1)\Sigma_a^F(0)[1 - \sigma_a^F\varepsilon\phi(0)t] - \Sigma_a^M - \frac{(\gamma^{\text{Te}} + \gamma^{\text{Xe}})\Sigma_f(0)\phi(0)}{\lambda^X/\sigma_a^X + \phi(t)} \\ - \gamma^{\text{Nd}}\Sigma_f(0)[1 - \varepsilon\sigma_a^F\phi(0)t] - \sigma_{\text{fp}'}\gamma_{\text{fp}'}\Sigma_f(0)\phi(0)t\end{aligned} \tag{6.26}$$

The soluble poison will be removed by the end of cycle, and the burnable poisons should be fully depleted by that time. Thus the lifetime, or cycle time, is the time at which the reactor can no longer be maintained critical with the control rods withdrawn as fully as allowed by safety considerations. This minimum

control cross section is small, and we set it to zero. The end-of-cycle time can be determined from Eq. (6.26) by setting $\Sigma_a^C = 0$ and solving for t_{EOC}:

$$t_{\text{EOC}} = \begin{cases} \dfrac{\eta\rho_{\text{ex}}(1+\alpha) - (\gamma^{\text{Te}}+\gamma^{\text{Xe}})\phi(0)\sigma_a^X/\lambda^X - \gamma^{\text{Nd}}}{[(\eta-1)(1+\alpha)\sigma_a^F - \gamma^{\text{Nd}}\sigma_a^F + \gamma_{\text{fp}'}\sigma_{\text{fp}'}]\phi(0)}, & \phi(t) \ll \dfrac{\lambda^X}{\sigma_a^X} \\ \dfrac{\eta\rho_{\text{ex}}(1+\alpha) - (\gamma^{\text{Te}}+\gamma^{\text{Xe}}+\gamma^{\text{Nd}})}{[(\eta-1)(1+\alpha)\sigma_a^F - (\gamma^{\text{Te}}+\gamma^{\text{Xe}}+\gamma^{\text{Nd}})\sigma_a^F + \gamma_{\text{fp}'}\sigma_{\text{fp}'}]\phi(0)}, & \phi(t) \gg \dfrac{\lambda^X}{\sigma_a^X} \end{cases} \tag{6.27}$$

where α is the capture-to-fission ratio for the fuel, and

$$\rho_{\text{ex}} \equiv \frac{k_\infty(0) - 1}{k_\infty(0)} \tag{6.28}$$

is the excess reactivity at beginning-of-cycle without xenon, samarium, fission products, or control cross section. The initial control cross section (including soluble and burnable poisons) must be able to produce a negative reactivity greater than ρ_{ex}. It is clear from Eq. (6.27) that the cycle lifetime is inversely proportional to the power, or flux, level.

6.5 FUEL REPROCESSING AND RECYCLING

A substantial amount of plutonium is produced by neutron transmutation of ^{238}U in LWRs. About 220 kg of fissionable plutonium (mainly ^{239}Pu and ^{241}Pu) is present in the spent fuel discharged from an LWR at a burnup of 45 MWd/T. The spent fuel can be reprocessed to recover the plutonium (and remaining enriched uranium) for recycling as new fuel.

Composition of Recycled LWR Fuel

The potential energy content of the fissile and fertile isotopes remaining in spent reactor fuel (Table 6.2) constitutes a substantial fraction of the potential energy content of the initial fuel loading, providing an incentive to recover the uranium and plutonium isotopes for reuse as reactor fuel. The recycled plutonium concentrations calculated for successive core reloads of a PWR are shown in Table 6.5. The initial core loading and the first reload were slightly enriched UO_2. The plutonium discharged from the first cycle was recycled in the third cycle, that in the second cycle in the fourth cycle, and so on, in separate mixed oxide (MOX) $UPuO_2$ pins. The proportion of MOX increases from about 18% in the second reload to just under 30% in the sixth and subsequent reloads, for which reloads the plutonium recovered from spent MOX and UO_2 fuel is about the same as was loaded into this fuel at beginning-of-cycle (i.e., the plutonium concentration reaches equilibrium). The percentage of plutonium in MOX increases from less than 5% on the initial recycle

load to about 8% in equilibrium, in order to offset the reactivity penalty

TABLE 6.5 Plutonium Concentrations in a PWR Recycling Only Self-Generated Plutonium (wt %)

Loading:	1	2	3	4	5	6	7
Recycle:			1	2	3	4	5
^{235}U in UO_2	2.14	3.0	3.0	3.0	3.0	3.0	3.0
Pu in MOX	—	—	4.72	5.83	6.89	7.51	8.05
MOX of fuel	—	—	18.4	23.4	26.5	27.8	28.8
^{235}U discharged	0.83	—	—	—	—	—	—
Discharged Pu							
^{239}Pu	56.8	56.8	49.7	44.6	42.1	40.9	40.0
^{240}Pu	23.8	23.8	27.0	38.7	29.4	29.6	29.8
^{241}Pu	14.3	14.3	16.2	17.2	17.4	17.4	17.3
^{242}Pu	5.1	5.1	7.1	9.5	11.1	12.1	12.9

Source: Data from Ref. 3; used with permission of Taylor & Francis/Hemisphere Publishing.

Physics Differences of MOX Cores

The use of MOX fuels in PWRs changes the physics characteristics in several ways. The variation with energy of the cross sections for the plutonium isotopes is more complex than for the uranium isotopes, as shown in Fig. 6.9. The absorption cross sections for the plutonium isotopes are about twice those of the uranium isotopes in

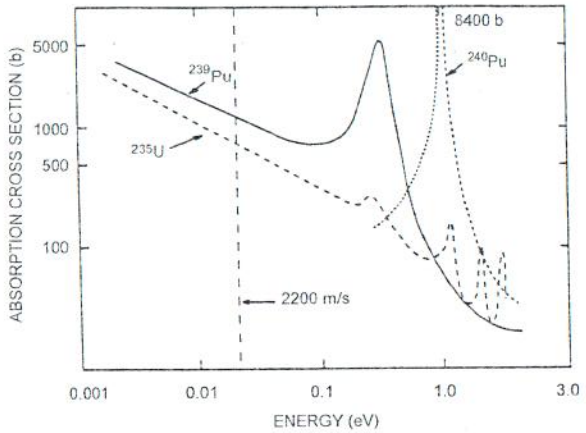

Fig. 6.9 Thermal absorption cross section for ^{239}Pu. (From Ref. 4; used with permission of American Nuclear Society.)

a thermal spectrum and are characterized by large absorption resonances in the epithermal (0.3 to 1.5 eV) range and by overlapping resonances. Representative thermal neutron spectra in UO_2 and MOX fuel cells are compared in Fig. 6.10.

Thermal parameters for ^{235}U and ^{239}Pu, averaged over a representative LWR thermal neutron energy distribution, are given in Table 6.6. Because of the larger thermal absorption cross section for ^{239}Pu, the reactivity worth of control rods

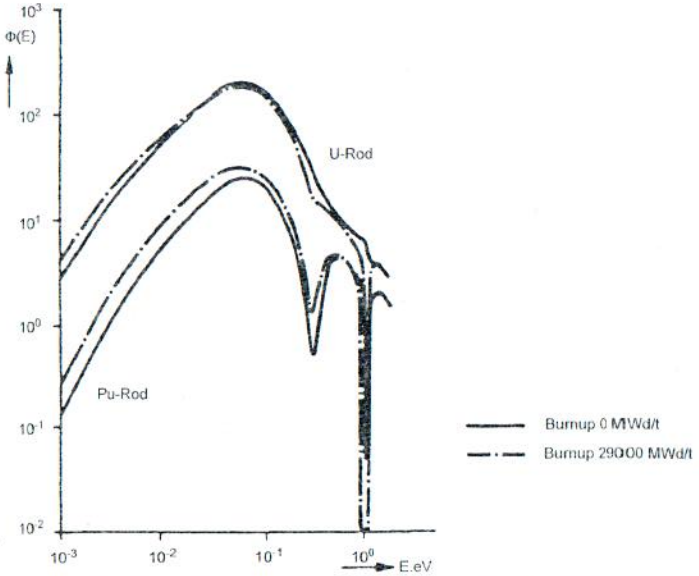

Fig. 6.10 Thermal neutron spectra in UO_2 and MOX PWR fuel cells. (From Ref. 1; used with permission of Nuclear Energy Agency, Paris.)

TABLE 6.6 Thermal Parameters for ^{235}U and ^{239}Pu in a LWR

Parameter	^{235}U	^{239}Pu
Fission cross section σ_f (barns)	365	610
absorption cross section σ_a (barns)	430	915
Nu-fission to absorption η	2.07	1.90
Delayed neutron fraction β	0.0065	0.0021
Generation time Λ (s)	4.7×10^{-5}	2.7×10^{-5}

Source: Data from Ref. 4; used with permission of American Nuclear Society.

burnable poisons, and soluble poisons (PWRs) will be less with MOX fuel than with UO_2, unless the MOX rods can be placed well away from control rods and burnable poisons. The higher ^{239}Pu fission cross section will lead to greater power peaking with MOX than with UO_2, unless the MOX rods are placed well away from water gaps.

There are reactivity differences between MOX and UO_2. The buildup of ^{240}Pu and ^{242}Pu with the recycling MOX fuel accumulates parasitic absorbers that results in a reactivity penalty, as discussed in Section 6.1. The average thermal value of η is less for ^{239}Pu than for ^{235}U, which requires a larger fissile loading to achieve the same initial excess reactivity with MOX as with UO_2. Furthermore, the temperature defect is greater for MOX because of the large low-energy resonances in ^{239}Pu and ^{240}Pu shown in Fig. 6.9. However, the reactivity decrease with burnup is less for MOX than for UO_2, because of the lower η for ^{239}Pu than for ^{235}U, and because of the transmutation of ^{240}Pu into fissionable ^{241}Pu, so that less excess reactivity is needed.

The delayed neutron fractions for ^{239}Pu, ^{241}Pu, and ^{235}U are in the ratio 0.0020/0.0054/0.0064, which means that the reactivity insertion required to reach prompt critical runaway conditions is less for MOX than for UO_2 by a factor that depends on the $^{239}Pu/^{241}Pu/^{235}U$ ratio. As the ^{241}Pu builds up with repeated recycle, the difference between MOX and UO_2 decreases. The neutron generation time is also shorter for MOX than for UO_2, so that any prompt supercritical excursion would have a shorter period. The fission spectrum neutrons are more energetic for ^{239}Pu than for ^{235}U. On the other hand, because of the large epithermal absorption resonances in the plutonium isotopes, the moderator and fuel Doppler temperature coefficients of reactivity tend to be more negative for MOX cores than for UO_2 cores. Accumulation of actinides, which are strong emitters of energetic alpha particles, leads to higher radioactive decay heat removal requirements with MOX. These considerations would tend to limit the MOX fraction in a reload core.

The yield of ^{135}Xe is about the same for the fission of plutonium as for the fission of uranium. Due to the higher thermal absorption cross section of the plutonium isotopes, the excess reactivity needed to start up at peak xenon conditions and the propensity for spatial flux oscillations driven by xenon oscillations (Chapter 16) are less in a MOX than a UO_2 core.

For plutonium recycle in other reactor types, similar types of physics considerations would enter. However, the different relative values of η for ^{235}U and ^{239}Pu in different spectra (e.g., the epithermal spectrum of a HTGR and the fast spectrum of a LMFBR) would lead to different conclusions about reactivity penalties. In fact, LMFBRs have been designed from the outset with the concept of switching from ^{235}U to ^{239}Pu as the latter was bred.

Physics Considerations with Uranium Recycle

Although it is relatively straightforward to separate uranium from other chemically distinct isotopes, it is impractical to separate the various uranium isotopes from

each other in the reprocessing step. So recycling uranium means recycling all of the uranium isotopes, some of which are just parasitic absorbers and another of which leads through subsequent decay to the emission of an energetic gamma.

Two isotopes present in relatively small concentrations in fresh fuel (^{234}U and ^{236}U) necessitate adding ^{235}U to enrich reprocessed uranium to a higher enrichment than is required with fresh uranium fuel. Uranium-234 has a large absorption resonance integral and, while only a tiny fraction in natural uranium, will tend to be enriched along with ^{235}U. Uranium-236 is produced by neutron capture in ^{235}U and by electron capture in ^{236}Np, as shown in Fig. 6.4, and is a parasitic neutron absorber with a significant capture resonance integral. Reprocessed uranium is made difficult to handle by the decay product ^{208}Tl, which emits a 2.6-MeV gamma with $t_{1/2} = 3.1$ min. This radioisotope is produced by a series of alpha decays of ^{232}U, which is produced by the chain shown in Fig. 6.4.

Physics Considerations with Plutonium Recycle

The same type of difficulties exists for plutonium reprocessing as discussed for uranium—all of the plutonium isotopes must be recycled. Plutonium-236 decays into ^{232}U, which leads to the emission of a 2.6-MeV gamma, as described above. Plutonium-238 is produced through neutron transmutation of ^{237}Np; it alpha-decays with $t_{1/2} = 88$ years and constitutes a large shutdown heat source if present in sufficient quantity. Plutonium-240 has an enormous capture resonance integral. Both ^{238}Pu and ^{240}Pu contribute a large spontaneous fission neutron source. Plutonium-241, while having a large fission cross section, also decays into ^{241}Am, which has a large thermal capture cross section and a large capture resonance integral. Americium-241 also decays into daughter products which are energetic gamma emitters. Stored plutonium loses its potency as a fuel over time because of the decay of ^{241}Pu into ^{241}Am. Plutonium from spent LWR fuel at a typical burnup of about 35,000 MWd/T must be utilized within 3 years after discharge or it will be necessary to reprocess it again to remove the ^{241}Am and daughter products.

Reactor Fueling Characteristics

Nuclear fuel cycles with plutonium recycle have been studied extensively (e.g., Ref. 1). Representative equilibrium fueling characteristics for LWRs operating on the ^{238}U–^{239}Pu and ^{232}Th–^{233}U fuel cycles and for a LMFBR operating on the ^{238}U–^{239}Pu fuel cycle are shown in Table 6.7. Fuel is partially discharged and replenished each year (*annual discharge* and *annual reload*), requiring a net amount of new fuel (*annual makeup*) from outside sources. In the absence of reprocessing and recycling, the annual reload would have to be supplied from outside sources. The LMFBR produces more fuel than it uses and could provide the extra fuel needed by the LWRs from the transmutation of ^{238}U if LMFBRs and LWRs were deployed in the ratio of about 7:5.

TABLE 6.7 Representative Fueling Characteristics of 1000-MWt Reactors

Characteristic	Reactor Type		
	LWR	LWR	LMFBR
Fuel cycle	^{232}Th–^{233}U	^{238}U–^{239}Pu	^{238}U–^{239}Pu
Conversion ratio	0.78	0.71	1.32
Initial core load (kg)	1,580	2,150	3,160
Burnup (MWd/T)	35,000	33,000	100,000
Annual reload (kg)	720	1,000	1,480
Annual discharge (kg)	435	650	1,690
Annual makeup (kg) (fresh)	285	350	(−210)

Source: Data from Ref. 8; used with permission of International Atomic Energy Agency.

6.6 RADIOACTIVE WASTE

Radioactivity

The actinides produced in the transmutation–decay of the fuel isotopes and the fission products are the major contributors to the radioactive waste produced in nuclear reactors, although activated structure and other materials are also present. The activity per ton of fuel for representative LWR and LMFBR discharges are given in Table 6.8. The fission products account for almost the entire radioactivity of spent fuel at reactor shutdown, but because of their short half-lives, this radioactivity level decays relatively quickly. In fact, the radioactivity of the spent fuel decreases substantially within the first 6 months after removal from the reactor, as shown in Table 6.8. The more troublesome fission products from the waste management point of view are those with long half-lives like ^{99}Tc ($t_{1/2} = 2.1 \times 10^5$ years) and ^{129}I ($t_{1/2} = 1.59 \times 10^7$ years) and those that are gamma emitters, such as ^{90}Sr and ^{137}Cs, which produce substantial decay heating. The actinides constitute a relatively small part of the total radioactivity at reactor shutdown but become relatively more important with time because of the longer half-lives of ^{239}Pu and ^{240}Pu and dominate the radioactivity of spent fuel after about 1000 years.

Hazard Potential

A simple, but useful, measure of the hazard potential of radioactive material is the *hazard index*, defined as the quantity of water required to dilute the material to the maximum permissible concentration for human consumption. The hazard index for spent LWR fuel is plotted against time after shutdown in Fig. 6.11. Fission products dominate the hazard index up to about 1000 years after shutdown, beyond which time the transuranics (actinides) become dominant. Including the plutonium in the recycled uranium fuel increases the hazard potential because of the continued buildup of ^{239}Pu and ^{240}Pu. Beyond 1000 to 10,000 years after shutdown

TABLE 6.8 Radioactivity of Representative LWR and LMFBR Spent Fuel at Discharge and at 180 Days (LWR) or 30 Days (LMFBR) After Discharge[a]

Nuclide	Half-Life $t_{1/2}$	Radiations[b]	Activity (Ci/tonne Heavy Metal)			
			LWR Fuel		LMFBR Fuel	
			Discharge	180 d	Discharge	30 d
^{3}H	12.3 y	β	5.744×10^{2}	5.587×10^{2}	1.648×10^{3}	1.640×10^{3}
^{85}Kr	10.73 y	β, γ	1.108×10^{4}	1.074×10^{4}	1.473×10^{4}	1.466×10^{4}
^{89}Sr	50.5 d	β, γ	1.058×10^{6}	9.603×10^{4}	1.333×10^{5}	8.939×10^{5}
^{90}Sr	29.0 y	β, γ	8.425×10^{4}	8.323×10^{4}	9.591×10^{4}	9.572×10^{4}
^{90}Y	64.0 h	β, γ	8.850×10^{4}	8.325×10^{4}	1.214×10^{5}	9.572×10^{4}
^{91}Y	59.0 d	β, γ	1.263×10^{6}	1.525×10^{5}	1.794×10^{6}	1.269×10^{6}
^{95}Zr	64.0 d	β, γ	1.637×10^{6}	2.437×10^{5}	3.215×10^{6}	2.340×10^{6}
^{95}Nb	3.50 d	β, γ	1.557×10^{6}	4.689×10^{5}	3.149×10^{6}	2.954×10^{6}
^{99}Mo	66.0 h	β, γ	1.875×10^{6}	3.780×10^{-14}	4.040×10^{6}	2.108×10^{3}
^{99m}Tc	6.0 h	γ	1.618×10^{6}	3.589×10^{-34}	3.487×10^{6}	2.002×10^{3}
^{99}Tc	2.1×10^{5} y	β, γ	1.435×10^{1}	1.442×10^{1}	3.278×10^{1}	3.293×10^{1}
^{103}Ru	40.0 d	β, γ	1.560×10^{6}	6.680×10^{4}	4.617×10^{6}	2.730×10^{6}
^{106}Ru	369.0 d	β, γ	4.935×10^{5}	3.519×10^{5}	2.248×10^{6}	2.125×10^{6}
^{103m}Rh	56.0 min	γ	1.561×10^{6}	6.686×10^{4}	4.619×10^{6}	2.733×10^{6}
^{111}Ag	7.47 d	β, γ	5.375×10^{4}	3.005×10^{-3}	2.294×10^{5}	1.422×10^{4}
^{115m}Cd	44.6 d	β, γ	1.483×10^{3}	9.042×10^{1}	7.041×10^{3}	4.418×10^{3}

(Continued)